Proteomic Characterization of Perisynaptic Astrocytes in Synaptic Plasticity

Carney, K.E.

2014

CHAPTER 4

Identification of astrocyte proteins involved in supraoptic nucleus structural plasticity during hyperosmosis and lactation

Karen E. Carney[1,2,3], Pim van Nierop[1], Roel C. van der Schors[1], Ka Wan Li[1], August B. Smit[1], Stéphane H.R. Oliet[2,3], Mark H.G. Verheijen[1]

[1] Dept. Molecular & Cellular Neurobiology, Center for Neurogenomics and Cognitive Research, Neuroscience Campus Amsterdam, VU University Amsterdam, Amsterdam, The Netherlands

[2] INSERM U862, Neurocentre Magendie, 33077 Bordeaux, France.

[3] Université de Bordeaux, 33077 Bordeaux, France

ABSTRACT

Astrocytes in the supraoptic nucleus (SON) of the hypothalamus demonstrate prominent temporary structural changes during physiological events such as dehydration and lactation. Such structural remodeling is characterized by a reduction in the astrocytic coverage of oxytocin neurons and their synapses, which contributes to the observed functional changes in synaptic activity during dehydration and lactation. In order to elucidate the underlying mechanisms of astrocytic contributions to synaptic plasticity we investigated the astrocyte protein expression profile for structural changes in the SON during lactation and hyperosmotic challenge. For this, SON from virgin, lactating, and hyperosmotic rats were collected from acute hypothalamic slices and analyzed by mass spectrometry to identify proteins differentially regulated by the changes in synaptic structure induced by lactation and hyperosmolarity. Our mass spectrometry data analysis placed particular focus on regulation of astrocyte-specific proteins. Immunoblotting was used to validate the mass spectrometry data. A reproducible up-regulation of Ndrg2 under both lactating and hyperosmotictic condition was detected, however, large discrepancies were found for most proteins. The difficulty to reproducibly find expression changes for SON proteins during SON structural remodeling might be explained by its rapid dynamic nature. We discuss possible modifications to the experimental design to enable successful identification of more astrocyte proteins involved in this structural plasticity.

INTRODUCTION

The supraoptic nucleus (SON) is part of the hypothalamic-neurohypophysial system. The SON is densely packed with vasopressin and oxytocin magnocellular neurons interspersed with thin astrocytic processes. The neuropeptide vasopressin is involved in the regulation of water balance whereas oxytocin primarily participates in the orchestration of reproductive processes including parturition and the milk ejection reflex, but has an additional role in water homeostasis [205-207]. Axons from the magnocellular neurons project through the internal layer of the median eminence directly to the neurohypophysis allowing oxytocin and vasopressin to be directly secreted into the blood stream upon physiological demand [208, 209].

The anatomical restructuring capacity of the supraoptic nucleus (SON) has been used as a model of structural and functional plasticity for decades [210, 211]. During conditions of physiological stimulation such as dehydration, hyperosmosis, and lactation, activation of the nucleus results in hypertrophy of neuronal somas and the retraction of the glial processes ensheathing synapses. This retraction allows for juxtaposition of more neuronal components, leading to the formation of additional synapses and even 'double synapses', where one axon terminal forms a synapse with two different post synaptic cells [212]. Interestingly, the structural remodeling and consequently increased number of double synapses, increased extent of neuronal apposition, and decreased percent of glial contact per neuron is observed only for oxytocin neurons, not vasopressin neurons. This remodeling is observed to equal extents in both hyperosmosis/dehydration and lactation [29, 30]. Additionally, this structural plasticity is complete reversible as after the end of lactation or upon rehydration the astrocytic coverage of neurons and number of synapses returns to normal [213, 214].

The reduced synaptic coverage also effectively removes the physical barrier between synapses, facilitating diffusion of all signaling molecules within the nucleus. This is particularly true for glutamate, whose uptake is delayed under stimulated conditions since transporters ensuring its clearance are located on the retracted astrocytic processes. Glial withdrawal thus causes a local buildup of the excitatory amino acid and consequently an enhanced activation of presynaptic group III metabotropic glutamate receptors (mGluRs) that are negatively coupled to glutamate release [106]. One of the main outcome of the reduced astroglial coverage is thus a reduced efficacy at excitatory inputs due to an enhanced negative feedback provided by glutamate onto its own release. The glial withdrawal also allows spillover of glutamate from one synapse to another, leading to functional alterations on distant terminals. Increased levels of synaptic glutamate after high levels of neuronal firing can diffuse and activate presynaptic group III mGluRs on neighboring GABAergic neurons, resulting in decreased inhibitory signals [93]. As glutamatergic volleys onto oxytocin neurons underlie the lactation-associated burst firing pattern required for the milk-ejection reflex [215], this disinhibition may serve to facilitate information transfer at highly-active synapses conveying lactation stimulus-related signals [105]. Additionally, retraction of astrocyte processes from the synapse decreases availability of the NMDA-receptor co-agonist D-serine, which is produced exclusively by astrocytes in the SON. Reduced D-serine levels alter the NMDA receptor activation probability, thus requiring higher levels of glutamatergic input (i.e volleys conveying lactation information) to induce potentiation of the synapse [107]. Together these consequences of astrocyte retraction establish a high-pass filter whereby only synchronized glutamatergic input from lactation stimulation will result in the oxytocin neuron burst firing sufficient to induce the milk-ejection reflex [216].

Several previous studies have sought to identify genes and proteins involved in the regulation of this dynamic process using models of dehydration, hyperosmosis, and/or lactation. For instance, poly-sialyated neuronal cell adhesion molecule (PSA-NCAM) was found highly expressed by perisynaptic astrocyte processes in the SON, and the presence of the PSA modification, which inhibits cell adhesion, was required for the induction of SON structural plasticity in both hyperosmosis and lactation models [217]. Microarray studies comparing the similarities of dehydration-induced transcriptome changes between mice and rats have reported regulation of genes involved in polyamine synthesis, prostaglandin E2 signaling, and extracellular matrix remodeling in both species, suggesting that evolutionarily conserved pathways are likely to be important to SON physiology [218-220]. Two-dimensional difference gel electrophoresis (2D-DIGE) proteomic analysis of dehydrated rat SON identified the regulation of 3 proteins by dehydration: heat-shock protein 1 alpha (Hsp1a), neuronal axonal membrane protein (NAP22), and protein-disulfide isomerase 3 (Pdia3). However, the mechanism via which these proteins could affect structural plasticity remains to be elucidated [221].

Each of these studies has contributed a piece to the puzzle but surprisingly there is very little overlap in the genes and proteins so far proposed to be involved in this dynamic process. This may be due to differences in experimental protocols, poor correlation between gene transcript levels and protein levels, and reported strain-dependent variations in rat hypothalamic-neurohypophyseal transcriptomes [222]. Here we set out for a more definitive answer about the underlying mechanisms of this remodeling, by performing a large-scale protein-level analysis in both lactation and hyperosmosis models. Because lactation and hyperosmosis are robust physiologically stimulating paradigms on their own, we

hypothesized that many proteins would change levels for each of the models, however, that proteins which are similarly regulated in both models would be most likely be involved in the structural plasticity, as this is shared between both conditions.

We thus conducted a label-free semi-quantitative mass spectrometry analysis of SON isolated from virgin, lactating, and hyperosmotic female rats. Clustering of the identified proteins, based on the patterns of expression-level changes, allowed us to identify groups of proteins that behaved similarly in both plasticity-inducing paradigms. Unfortunately, we were unable to validate most of the mass spectrometry results by immunoblotting. Further analyses suggested that our selected approach likely contained too much biological and technical variation to achieve the desired aims. However, the overall principle of the experiment is likely to remain valid and with some modifications to the experimental design, this approach is promising for identification of astrocyte-proteins involved in SON structural plasticity.

RESULTS

Mass spectrometry analysis of SON from virgin, hyperosmotic, and lactating rats

To identify SON proteins regulated by plasticity, a crude membrane fraction (P2+M) was isolated from the supraoptic nuclei of a pool of 3 female rats of either the virgin, hyperosmotic, or lactating rats. Four samples of each group were analyzed by label free quantification on an Orbitrap mass spectrometer. A total of 3363 proteins were detected that met the requirement of having peptides present in at least 2 samples. To determine if any proteins were significantly regulated, all 3363 proteins were subjected to statistical analysis with SAM to generate false-discovery rates (FDRs). The FDRs allows one to estimate the level

of false-discoveries (incorrectly rejected null hypotheses) present in a subset of the data, and enables one to select a collection of proteins that are consistent with a desired level of false-discoveries. Because we were interested in conducting a large-scale screen to identify many possible targets and associated changes in biological function, we accepted a relatively high false discovery rate (FDR) of 22% for our statistical analyses. Multiclass analysis of all 3 groups resulted in 985 proteins regulated with a false discovery rate (FDR) of 22% or less (Figure 1A). We also conducted a pairwise statistical analysis for virgin versus hyperosmotic and virgin versus lactating. A total of 1,040 proteins were different between hyperosmotic and virgin with a FDR of 21% while only 48 were different between lactating and virgin at 30% FDR (Figure 1 B, C). Protein numbers between these 3 groups were compared at slightly different FDRs because FDRs are generated in a step-wise rather than continuous fashion, thus it is often not possible to compare exactly the same FDR between different analyses.

The striking difference in numbers of proteins regulated in hyperosmotic versus lactating samples led us to further investigate the sample clustering patterns. Virgin, hyperosmotic, and lactating samples were clustered as groups as well as by individual samples using Pearson correlation coefficient-derived distance. Group clustering confirmed that virgin and lactating groups were much more similar to each other than they were to the hyperosmotic group, indicating the hyperosmotic protocol is a more robust model (Figure 1D). Clustering of the individual samples revealed 2 primary sub-clusters (Figure 1E). Hyperosmotic samples form a distinct, tight sub-cluster and virgin samples form a separate sub-cluster. However, half of the lactating samples clustered with hyperosmotic samples and the other half grouped with virgin samples. This high degree of variation between lactating samples may explain the low number of significantly regulated proteins between virgin and lactating groups.

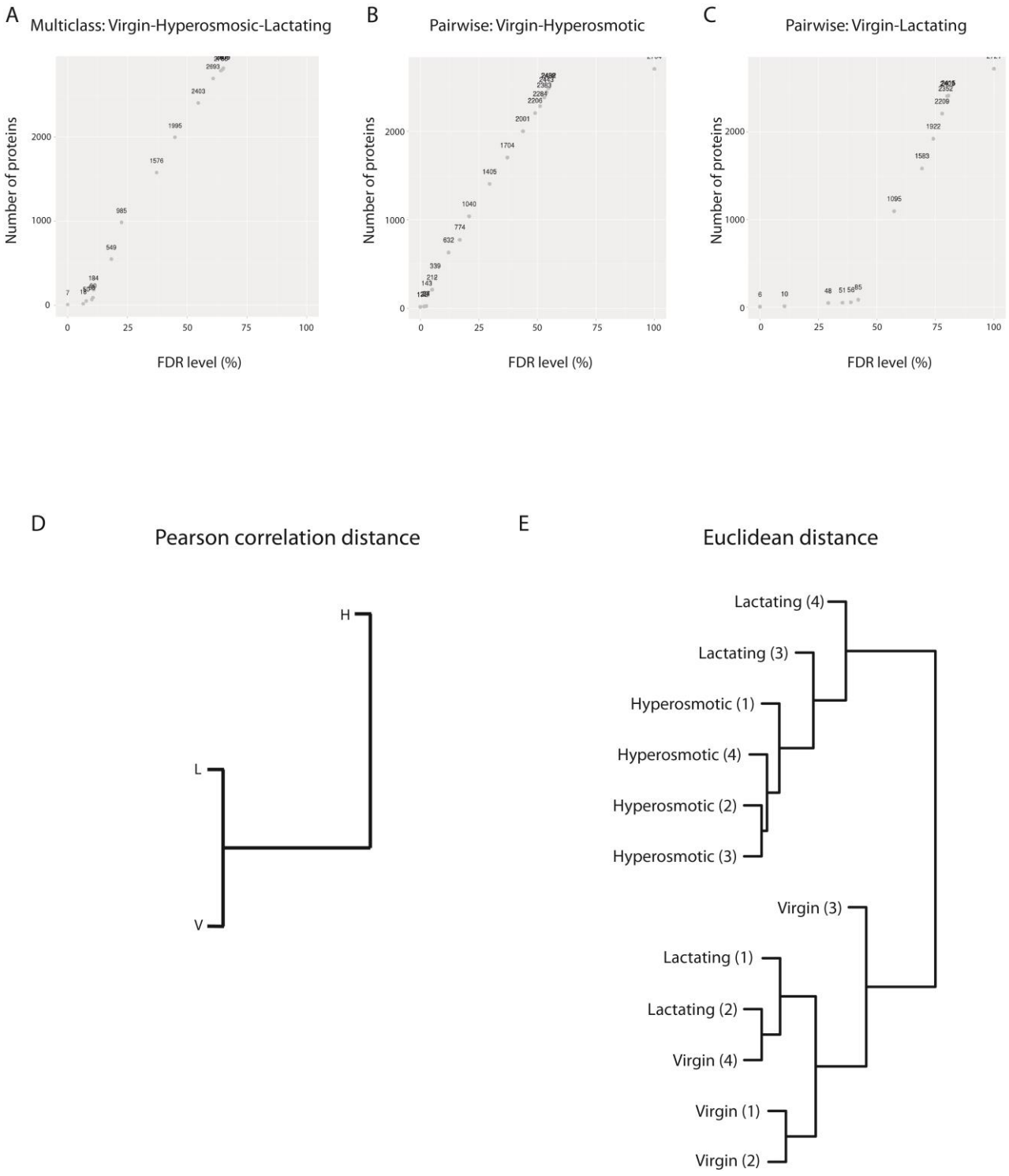

Figure 1: **Data quality analysis of SON from virgin (V), hyperosmotic (H), and lactating (L) rats analyzed by Orbitrap label-free mass spectrometry**. A) Number of proteins per false-discovery rate (FDR) level in the multiclass analysis. B) Number of proteins per FDR in the pair-wise virgin-hyperosmotic comparison. C) Number of proteins per FDR in the pair-wise virgin-lactating comparison. D) Clustering of experimental groups based on protein intensity using

Pearson correlation distance. E) Cluster of individual samples based on protein intensity using Euclidean distance.

Identification of clusters of plasticity-related protein regulations

In this paradigm we expect five possibilities for patterns of protein regulation: 1) proteins that are not regulated at all, and thus not present in the list of significantly regulated proteins, 2) proteins regulated in only the hyperosmotic, or 3) proteins regulated in only the lactating condition, thus not related to a plasticity mechanisms shared by both conditions, 4) proteins differentially regulated in each experimental model, and most importantly, 5) proteins regulated in the same direction in both paradigms and therefore possibly involved in the SON structural remodeling that occurs in both conditions (Figure 2A). In order to elucidate the proteins which were most likely to be plasticity-related, we used Euclidean distance to cluster all 985 proteins regulated at 22% FDR in the multiclass analysis. A total of 16 clusters were generated with each colored line representing the average expression level of a single protein across virgin, hyperosmotic, and lactating samples (Figure 2B). From these 16 clusters, we selected the 8 that exhibited a pattern most indicative of a role in plasticity (578 proteins). Clusters demonstrating increased expression in both hyperosmotic and lactating rats compared with virgins (green boxes, 329 proteins) were termed “up-regulated clusters” whereas those with decreased expression compared with virgins were designated as “down-regulated clusters” (red boxes, 249 proteins).

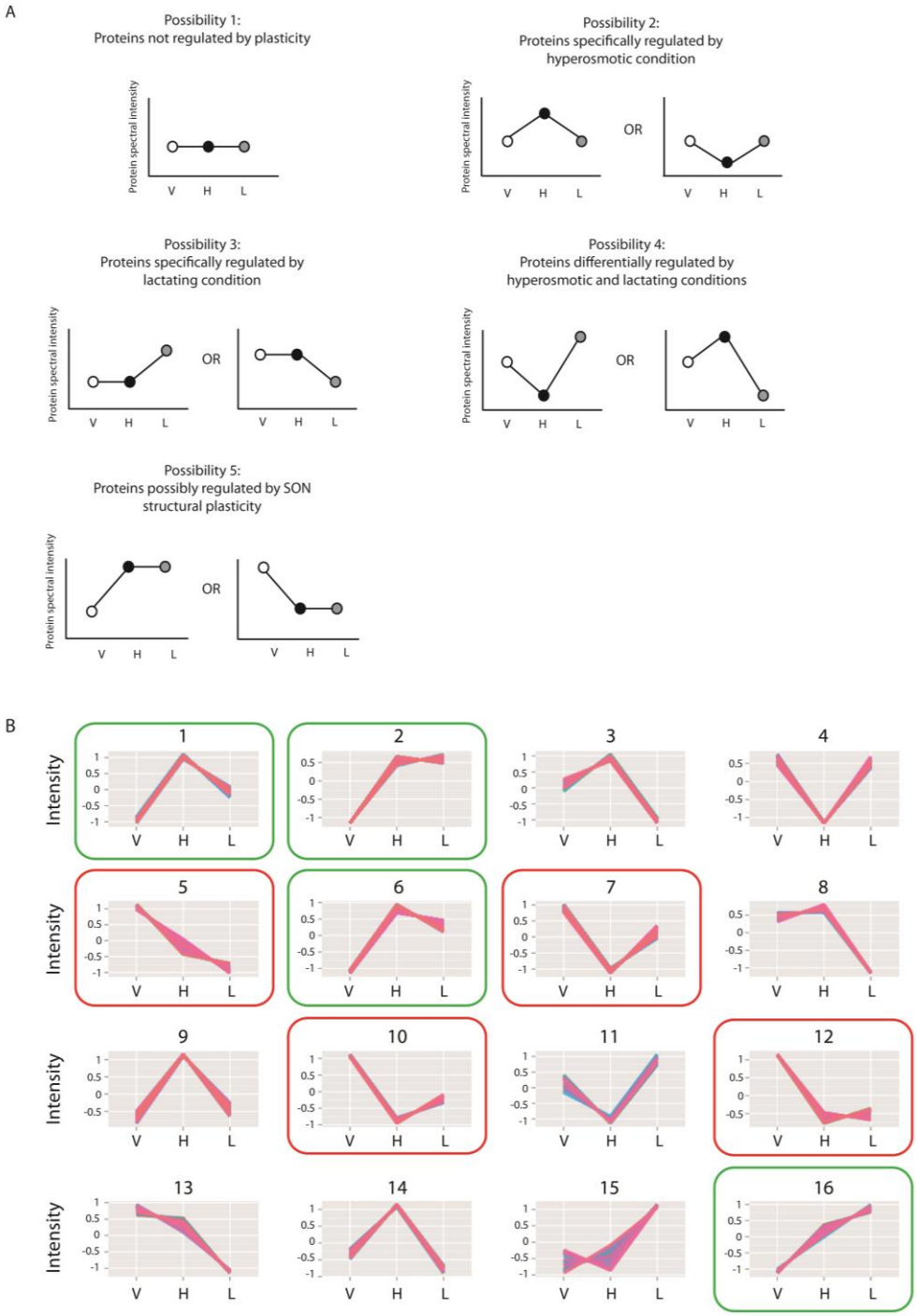

Figure 2: **Protein clustering for selection of plasticity-related proteins.** A) Expected expression pattern of proteins not regulated by hyperosmotic or lactating condition, regulated only by hyperosmotic condition, regulated only by lactating condition, differentially regulated by hyperosmotic and lactating conditions, and regulated by hyperosmotic and lactating conditions in the same direction, indicating a possible role in structural plasticity. B) Clustering of 985 significantly regulated (FDR ≤ 22%) proteins by Pearson correlation distance of summed peptide intensity into 16 clusters. Each colored line represents the expression pattern of a single protein. Clusters in green boxes ("up-clusters") and clusters in red boxes ("down-clusters") represent groups of proteins regulated by SON functional plasticity.

Distinguishing the contribution of astrocytes to SON plasticity

Our primary interest is in the role of astrocytes in plasticity. Because our analysis was performed on a membrane fraction from all cell types present in the SON, an additional level of filtering was required to determine which of these proteins are of astrocytic origin. To this end, the list of plasticity proteins was overlapped with a manually curated list of 1998 astrocyte–enriched genes [191], which resulted in the identification of 86 astrocytic plasticity proteins (Figure 3).

To further characterize these astrocyte proteins, a gene ontology over-representation analysis for biological process was performed. 'Small molecule metabolic process' was the most significant term, which contained many transmembrane transporters (including those for GABA, water, choline, and neutral amino acids). In addition, overrepresentation was found for multiple metabolic functions including carboxyl acid and lipid metabolism (Table 1).

Figure 3: **Schematic of proteomic data analysis towards identification of astrocyte-specific structural plasticity related proteins.**

Validation of mass spectrometry results by immunoblotting

Astrocyte proteins

Astrocyte plasticity proteins from the over-represented GO terms 'small molecule metabolic process', 'lipid metabolic process', and 'transport' were selected for validation of mass spectrometry results. Protein expression levels were evaluated in 5 independent samples from each experimental group.

For the proteins aldolase C (Aldoc) and Na^+-K^+ transporting ATPase subunit alpha 2 (Atp1a2), both present in the 'small molecule metabolism', mass spectrometry analysis predicted that both proteins should be up-regulated by plasticity conditions. However, immunoblots did not confirm the regulations for Atp1a2 ($F_{(2,12)}$ = 0.50, p= 0.62) or Aldoc ($F_{(2,12)}$ = 2.36, p = 0.14), although Aldoc regulations were in the correct direction (Figure 4A). Also for the 'lipid metabolic process' protein lipid phosphate phosphohydrolase 3 (Ppap2b) immunoblots did not confirm the up-regulation by plasticity ($F_{(2,12)}$ = .05, p = 0.95). 'Transport' proteins aquaporin 4 (Aqp4), Intersectin1 (Itsn1), and GABA-transporter 3 (GAT3) immunoblots also did not match the mass spectrometry results. However, GAT3 regulations were border-line significant ($F_{(2,12)}$ = 3.19, p= 0.07) and showed a strong trend toward up-regulation by hyperosmosis (1.14 –fold, p = 0. 03) and lactation (1.11 –fold, p = 0.09) which would be in line with the mass spectrometry data. Regulation of Aqp4 was significant ($F_{(2,12)}$ = 4.10, p= 0.05), but in disagreement with the mass spectrometry results as Aqp4 expression by immunoblot was down-regulated in hyperosmotic compared with both virgin (-1.20 -fold, p = 0.04) and lactating (1.23-fold, p = 0.03) animals. Thus, we were not able to satisfactory validate the mass spectrometry results for astrocyte proteins.

Table 1: Over-represented biological process terms in astrocyte-enriched plasticity cluster proteins

GO-ID	p-value	Count	%	Description	Genes in test set
44281	2.32E-07	27	2.1	small molecule metabolic process	PYCRL, ECH1, IMPA1, ACADS, ALDOC, ATP5B, SARS, CS, OGDHL, FDXR, ACOT1, ATP1A2, AMPD2, PSPH, PNPLA8, ACSS1, HMGCS2, PLCG1, ATG7, GPX4, AKR1B1, GCSH, AHCYL1, GK, ACSL6, PCCA, DUT
51179	2.17E-04	32	1.3	localization	SLC38A3, SLC44A2, SLC6A1, AP2S1, ATP5B, TRAPPC2L, ASTN1, AP3S1, AQP4, ITSN1, UQCRQ, SRC, CD44, COPB1, ATG7, AGT, SLC4A4, ACSL6, RILP, SLC6A11, CKAP5, FDXR, SPIRE1, ATP1A2, DBI, ITGA6, PLCG1, RAB35, NTRK2, RAB22A, CDC42BPA, RHOT2
51234	3.01E-04	29	1.3	establishment of localization	SLC38A3, SLC44A2, SLC6A1, AP2S1, ATP5B, TRAPPC2L, AP3S1, AQP4, ITSN1, UQCRQ, SRC, COPB1, ATG7, AGT, SLC4A4, ACSL6, RILP, SLC6A11, CKAP5, FDXR, SPIRE1, ATP1A2, DBI, PLCG1, RAB35, NTRK2, RAB22A, CDC42BPA, RHOT2
6810	5.41E-04	28	1.3	transport	SLC38A3, SLC44A2, SLC6A1, AP2S1, ATP5B, TRAPPC2L, AP3S1, AQP4, ITSN1, UQCRQ, SRC, COPB1, ATG7, AGT, SLC4A4, ACSL6, RILP, SLC6A11, CKAP5, FDXR, SPIRE1, ATP1A2, DBI, PLCG1, RAB35, NTRK2, RAB22A, RHOT2
19752	5.41E-04	13	2.5	carboxylic acid metabolic process	PYCRL, PNPLA8, ACSS1, ECH1, ACADS, SARS, ATG7, CS, GCSH, ACOT1, PSPH, ACSL6, PCCA
43436	5.41E-04	13	2.5	oxoacid metabolic process	PYCRL, PNPLA8, ACSS1, ECH1, ACADS, SARS, ATG7, CS, GCSH, ACOT1, PSPH, ACSL6, PCCA
6082	5.41E-04	13	2.5	organic acid metabolic process	PYCRL, PNPLA8, ACSS1, ECH1, ACADS, SARS, ATG7, CS, GCSH, ACOT1, PSPH, ACSL6, PCCA
42180	5.59E-04	13	2.4	cellular ketone metabolic process	PYCRL, PNPLA8, ACSS1, ECH1, ACADS, SARS, ATG7, CS, GCSH, ACOT1, PSPH, ACSL6, PCCA
9987	6.82E-04	62	0.7	cellular process	IMPA1, STAT5A, ATP5B, AP2S1, OGDHL, TRAPPC2L, PRDX4, GABBR1, AQP4, AP3S1, ACOT1, ITSN1, PSPH, UQCRQ, ACSS1, CD44, GPX4, COPB1, ATG7, KHDRBS1, AIFM1, ACADS, SARS, SPIRE1, PIGS, ST13, PNPLA8, PCCA, PYCRL, ECH1, EPDR1, ADCYAP1R1, ALDOC, ASTN1, SRC, SEC63, AGT, DMD, GCSH, NDRG2, PPAP2B, ACSL6, RILP, CKAP5, CS, FDXR, ATP1A2, AMPD2, DBI, ITGA6, HMGCS2, PLCG1, RAB35, AKR1B1, NTRK2, RAB22A, CDC42BPA, RHOT2, AHCYL1, GK, FABP7, DUT
6629	2.02E-03	14	2.0	lipid metabolic process	IMPA1, ECH1, ACADS, ATP5B, FDXR, ACOT1, PIGS, DBI, PNPLA8, HMGCS2, PLCG1, PPAP2B, PCCA, ACSL6
9991	2.91E-03	10	2.6	response to extracellular stimulus	ITGA6, HMGCS2, CD44, ACADS, ATG7, STAT5A, PSPH, DBI, ACSL6, SRC
16192	2.91E-03	11	2.4	vesicle-mediated transport	PLCG1, RAB35, COPB1, AP2S1, ATP5B, RAB22A, TRAPPC2L, AP3S1, SPIRE1, ITSN1, SRC

Proteins with low FDR or high fold changes

For most of the astrocyte proteins we attempted to validate, fold changes were < 2 with 22% FDR. To explore the possibility that validation failed because the measurements were too uncertain, we next blotted for proteins with low FDRs or high fold-changes. The mass spectrometry results were sorted by FDR and fold change, and high ranking proteins, for which an antibody was available, were selected for immunoblot analysis. (Figure 4B). Ezrin was measured by mass spectrometry to show a 2.9 -fold increase (45% FDR) in the hyperosmotic condition. By immunoblot analysis ezrin regulation was significant ($F_{(2,12)} = 4.75$, $p = 0.03$), but the regulation was opposite of the mass spectrometry results with a decrease in ezrin expression between virgin and lactating samples (-1.19 -fold, $p = 0.01$). The protein receptor-type tyrosine-protein phosphatase F (Ptprf) had a 0% FDR in the MS results and was detected in virgin condition samples, though not in any hyperosmotic or lactating condition samples, suggesting a strong decrease in expression by plasticity. Immunoblot analysis showed no difference in expression levels of this protein in any condition ($F_{(2,12)} = 0.55$, $p = 0.59$). Thus, we were also not able to satisfactory validate the mass spectrometry results for proteins with low FDR or high fold changes.

Proteins regulated only by hyperosmosis

Our initial bioinformatics analysis indicated that very few proteins were significantly regulated by lactation, so perhaps including all these samples in our multiclass analysis masked true changes present in the more robust virgin-hyperosmotic comparison. To determine whether we could validate any proteins regulated by only hyperosmosis we selected proteins with FDRs less than 10% in the virgin-hyperosmotic pairwise comparison, regardless of their degree of astrocyte expression. Protein disulfide isomerase (PDI), Claudin-11 (Cldn11), and

vesicle-fusing ATPase (NSF) were expected to be up-regulated by hyperosmosis, but immunoblotting showed no significant difference between groups (PDI: $F_{(2,9)} = 0.12$, $p = 0.88$; Cldn11: $F_{(2,12)} = 0.18$, $p = 0.83$; NSF: $F_{(2,12)} = 0.27$, $p = 0.27$). N-myc downstream regulated gene 2 (Ndrg2), an astrocyte-specific gene, was predicted by mass spectrometry to be 1.7-fold up-regulated by hyperosmosis with an 8% FDR. Immunoblotting confirmed Ndrg2 regulation ($F_{(2,9)} = 4.87$, $p = 0.03$) with a 1.4 fold increase in expression by hyperosmosis ($p = 0.02$), as well as a 1.4-fold increased expression in lactating samples ($p = 0.02$), suggesting it has a possible role in SON plasticity (Figure 4C).

Validation using mass spectrometry samples

Because validation of the mass spectrometry results on independent samples was generally unsuccessful, we attempted to confirm the regulations with immunoblotting on the same samples as were used for mass spectrometry analysis. This would indicate a possible problem with the independent replicates or potential complications with mass spectrometry data acquisition. Blotting for Ndrg2, GAT3, and Itsn1 on the same samples analyzed by mass spectrometry did not confirm the mass spectrometry results (Ndrg2: $F_{(2,9)} = 2.99$, $p = 0.10$; GAT3: $F_{(2,9)} = 0.44$, $p = 0.66$; Itsn1: $F_{(2,9)} = 0.54$, $p = 0.60$), although Ndrg2 showed a trend towards regulation with increased expression in lactating animals (1.34 –fold, $p = 0.05$) as was observed in the independent samples (Figure 5A). These results indicate that the protein lists generated with mass spectrometry do not accurately reflect the true protein content of the samples analyzed.

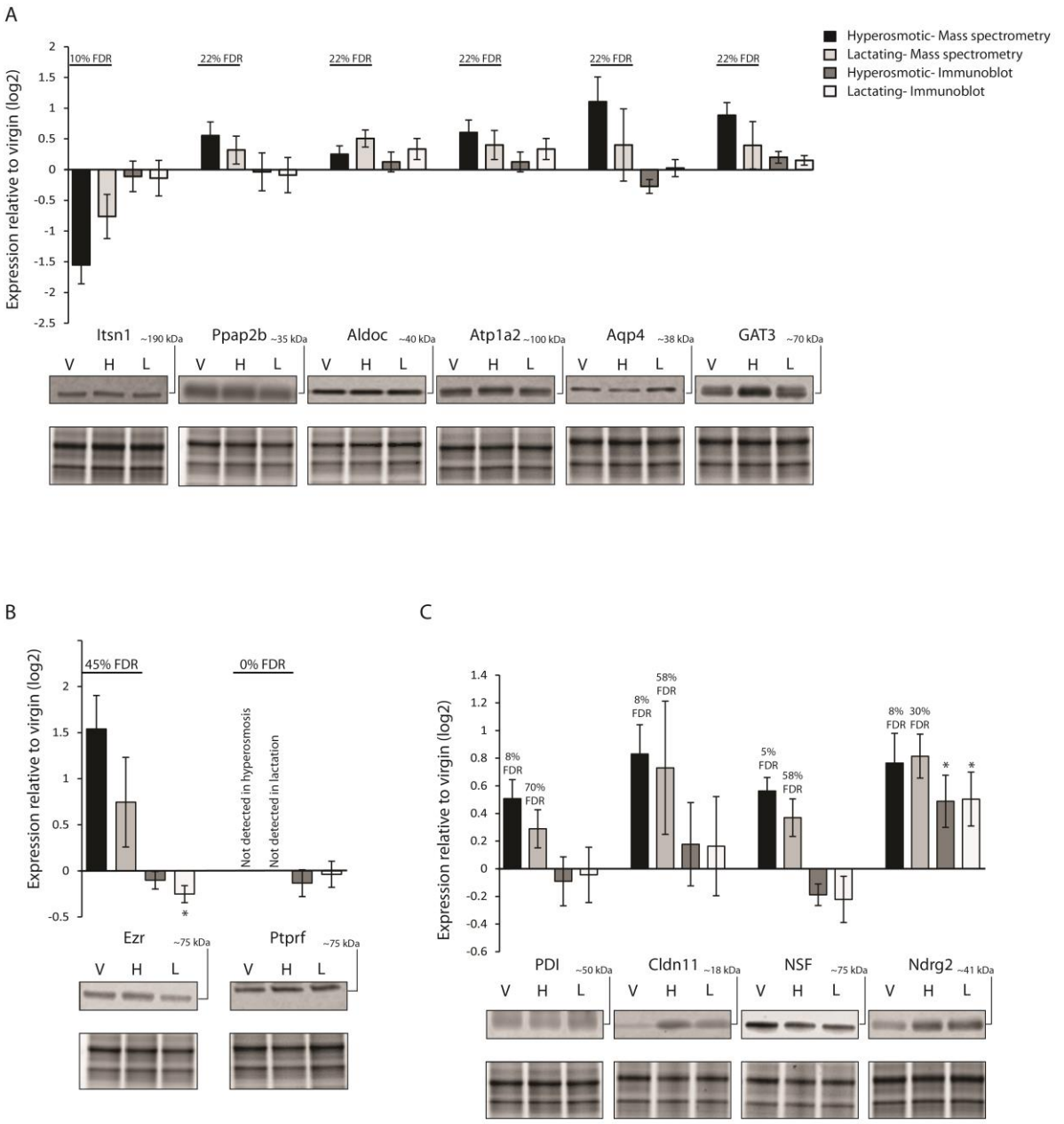

Figure 4: Immunoblot validation of mass spectrometry results. Shown are immunoblots of independent replicates for proteins that were significantly regulated with depicted FDR ≤ 22% in mass spectrometry. Representative immunoblots with approximate molecular weights and loading controls appear below the corresponding bar graph quantification for A) Depicted astrocyte-enriched proteins. Aqp4 was down-regulated by hyperosmosis with immunoblot analysis. B) Depicted high-fold change protein Ezrin and low FDR protein Ptprf. Ezrin expression was significantly down-regulated in lactating animals. C) Depicted proteins significantly regulated only in the hyperosmotic condition. Independent samples confirmed a significant up-regulation for Ndrg2 in both hyperosmotic and lactating rats. Bar graphs depict the mean log2 expression ratio relative to virgin samples ±SEM. * $p \leq 0.05$.

Proteins known to be regulated by SON plasticity

As a final validation step we wanted to assess whether our samples, regardless of mass spectrometry results, are in accordance with the literature regarding protein level changes that have previously been observed after SON stimulation. Protein disulfide isomerase A3 (Pdia3/GRP58) was previously found to be significantly up-regulated in the SON after 3 days of dehydration [221]. Although our mass spectrometry results also suggested an increase in Pdia3 after SON stimulation, we were unable to validate this finding by immunoblotting ($F_{(2,12)}$ = 0.91, p = 0.43, Figure 5B). Tyrosine hydroxylase is considered a marker of vasopressin neuron activation and increased expression levels are seen in the SON upon osmotic challenge [223]. Whereas tyrosine hydroxylase was not reliably detected with mass spectrometry, immunoblotting for tyrosine hydroxylase showed a significant regulation ($F_{(2,12)}$ = 5.02, p = 0.02), however, this was for a decrease in expression in hyperosmotic compared with virgin rats (-1.92 –fold, p = 0.009) with a trend toward reduction in lactating compared with virgin rats (1.52 –fold, p = 0. 07, Figure 5B).

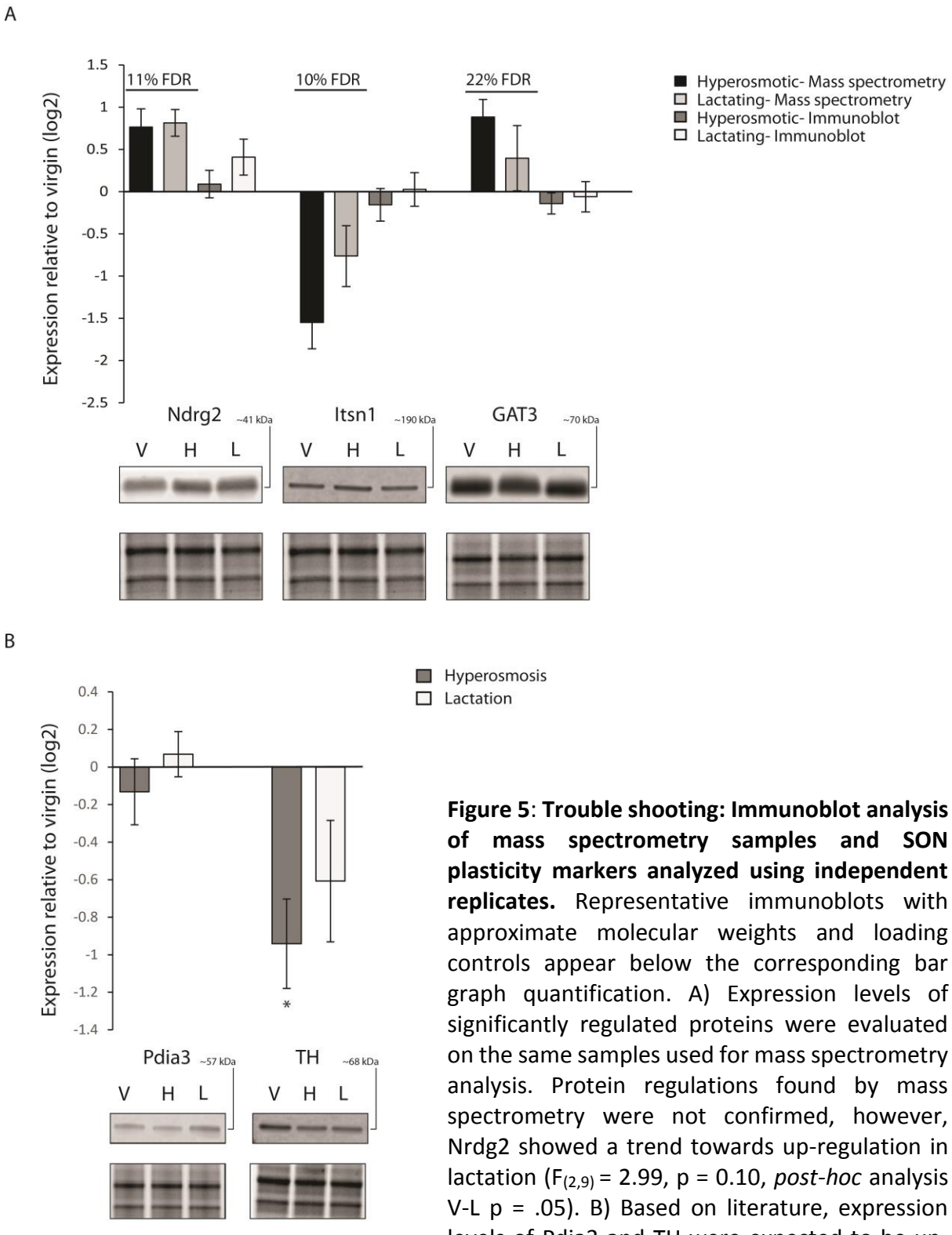

Figure 5: **Trouble shooting: Immunoblot analysis of mass spectrometry samples and SON plasticity markers analyzed using independent replicates.** Representative immunoblots with approximate molecular weights and loading controls appear below the corresponding bar graph quantification. A) Expression levels of significantly regulated proteins were evaluated on the same samples used for mass spectrometry analysis. Protein regulations found by mass spectrometry were not confirmed, however, Nrdg2 showed a trend towards up-regulation in lactation ($F_{(2,9)} = 2.99$, $p = 0.10$, *post-hoc* analysis V-L $p = .05$). B) Based on literature, expression levels of Pdia3 and TH were expected to be up-regulated in both plasticity conditions. TH was significantly down-regulated by plasticity compared with virgin animals. Bar graphs depict the mean log2 expression ratio relative to virgin samples ±SEM. * $p \leq 0.05$.

DISCUSSION

Plasticity-related proteins in the SON

To discover novel astrocyte proteins involved in structural plasticity we selected the well-known model of function-dependent plasticity in the supraoptic nucleus. Crude membrane fractions from SON of virgin, lactating, and hyperosmotic animals were analyzed by mass spectrometry to identify proteins which were regulated in the same direction in both experimental paradigms. To our knowledge, this is the first large-scale proteomics screen comparing both hyperosmotic and lactating animals using a label-free quantitation approach. A total of 578 proteins meeting the plasticity-related expression profile were considered for further analysis.

One protein, n-myc downstream-regulated gene 2 (Ndrg2), showed up-regulations in hyperosmotic and lactating animals by both mass spectrometry and immunoblotting. Ndrg2 has been identified as an astrocyte-specific protein expressed in the cell body as well as in the perisynaptic astrocyte processes [224]. Although its exact functions remain largely unknown, expression levels of Ndrg2 in astrocytes have been shown to increase with exposure to estrogen [225]. Remarkably, we found increased levels of Ndrg2 in the post-partum period, when estrogen levels are known to drop [226, 227]. Expression levels of Ndrg2 have also been shown to affect astrocyte process morphology, with decreased Ndrg2 expression resulting in reduced process length [228]. Although the percentage of neural soma profiles ensheathed by astrocyte processes is decreased during hyperosmosis and lactation, the absolute length of glial processes is actually increased due to the hypertrophy of mangocellular neurons [29, 30]. Therefore, the increased expression of Ndrg2 and probable increase in astrocyte process

length is in line with the structural changes induced by SON stimulation, suggesting Ndrg2 may facilitate these morphological rearrangements.

However, it should be noted that although the morphological plasticity of the stimulated SON is often referred to as “glial retraction”, it is not yet known if astrocytes actively retract from their neuronal contacts. Vassopressin neurons in the SON also hypertrophy during stimulation, but the percentage of their surface covered by glia processes remains the same as glial membrane extend to compensate neuronal swelling [29, 30]. This may suggest that the glial processes ensheathing oxytocin neurons fail to extend in response to neuronal hypertrophy rather than actively retract, and thus should be thought of more generally as astrocyte reorientation [229].

Sources of variation in the experimental paradigm

Although we found many significant regulations by mass spectrometry between virgin and hyperosmotic animals, few were identified between virgin and lactating animals. These data suggest hyperosmosis is a considerably more robust paradigm than lactation. Furthermore, this indicates that the use of virgin and lactating rats from different companies (Charles River and Harlan, respectively) did not result in noticeable SON proteome changes. However, most of the regulations that were measured could not be validated using immunoblotting on independent replicates or on the same replicates used for mass spectrometry analysis. Similarly, regulation of positive control proteins (Pdia3 and TH) also could not be confirmed by immunoblotting. Mass spectrometry analysis detected increased levels of Pdia3 in both hyperosmotic and lactating rats (multiclass FDR 18%), which is in accordance with the literature using a model of dehydration [221], although immunoblot analysis did not confirm this up-regulation. However, because dehydration is a more complex stimulus than

hyperosmosis, involving both hypertonicity and hypervolemia, the lack of up-regulation in our model may indicate that Pdia3 regulation is specific to hypervolemia. Additionally, the reported up-regulation of the cytosolic protein TH by hyperosmosis had been assesses by immunohistochemistry [230]. As we conducted immunoblot analyses on samples enriched for membrane proteins, the levels of TH present may not accurately represent the original cell contents. Nonetheless, overall we found poor correlation between mass spectrometry and immunoblot data. This indicates that a high degree of variation was present in our experimental paradigms and/or technical approaches, which may underlie the non-reproducible and conflicting results.

Temporal variation

Recent reports have indicated that protein expression level changes in the SON can happen in a matter of minutes [231-233]. Acute brain slices exposed to hyposmotic medium showed a dramatic increase in GFAP proteins levels in the SON already at 5 minutes after exposure, which had returned to normal after 20 minutes [233]. The same pattern was observed in rats given i.p. water injections to reduce osmolality, with GFAP levels peaking after 10 minutes and returning to baseline after 30 minutes [233]. Chronically dehydrated rodents show a decrease in GFAP expression, which returns to baseline upon rehydration [234], indicating expression level differences occur between different models of SON plasticity, but that these changes can happen rapidly.

Osmoregulatory mechanisms of the body strive to maintain stable levels of extracellular fluid osmolarity. However, fluctuations around this set-point occur as a result of daily variations in fluid intake, natriuresis, and perspiration [56]. Consumption of hyperosmotic solution induces a small fluctuation in portal venous osmolarity, and subsequently a compensatory activation

of the SON, mediated in part by activation of oxytocin magnocellular neurons [207, 235]. Activation of the SON and stimulation of oxytocin release with each fluctuation in blood osmolarity may require induction of structural plasticity mechanisms and concomitant alterations in protein expression. Because we did not monitor how long after their last water consumption the rats were sacrificed, the protein regulations observed may not correlate to the model as expected. Similarly, rapid changes in protein expression have been documented for the SON of lactating animals. GFAP expression during the suckling period significantly decreases within minutes, but returns to baseline levels after the milk-ejection reflex has occurred [231]. As we did not monitor the precise timing of each nursing before sacrificing the lactating mothers, this may have resulted in variation between the lactating rats for acute suckling-mediated changes in the SON. Together these observations suggest that rapid changes in protein level expression can occur with fluctuation in osmolarity and lactation timing that may be overlooked if the time of animal sacrifice is not closely monitored.

It should be noted, however, that electron microscopy has shown an approximately 10% decrease of astrocytic coverage of SON neurons during lactation and dehydration, indicating there is some level of constant structural difference between virgin/euhydrated animals and stimulated animals [29, 30]. The effects of this structural plasticity can also be detected by functional assays [106, 107]. The electron microscopy studies may represent a snapshot of an even more dynamic anatomical remodeling process that occurs *in vivo*, which is dependent on de novo protein synthesis [236]. Proteins with stably altered expression levels by stimulation, like Ndrg2, may represent permissive factors to the required dynamic changes.

Subcellular fractionation technique

Due to the small size of the SON, we were required to process samples into a crude membrane fraction rather than a more purified synaptosomal fraction. The use of a P2+M fraction may have masked protein level changes present specifically at the synapse (including perisynaptic astrocyte processes), which might have been detected when using sucrose-isolated synaptosomes (Chapter 3). On the other hand, with less astrocytic coverage during stimulation conditions it is possible that astrocytic PAP proteins would be well detected in synaptosomes from virgin samples, but less so in hyperosmotic or lactating animals. To investigate expression level changes of membrane proteins present in other cellular compartments, besides the nucleus, a P2+M fraction seems a viable choice.

SON dissection

Because the SON is located immediately adjacent to the optic chiasm it is easily identifiable in an acute slice preparation and can be dissected out using the punch technique [232, 237]. However, a drawback of the punch dissection technique is that small pieces of neighboring hypothalamic nuclei or myelinated tracts from the optic chiasm may also be included in the sample, which will contaminate the SON protein content, and may do so with variable extent between samples. Even when mass spectrometry analysis is conducted optimally, variation in the input material will disrupt the extraction of biologically relevant regulations from the resulting dataset, and these regulation are unlikely to be reproduced on independent replicates.

Utilization of the punch technique also results in inclusion of material from all cell types. Consequently, the heterogeneity of the sample means any cell-type specific protein regulation will be diluted and possibly become undetectable. The ability to sort specific cell-

types from the tissue, possibly using fluorescence- or magnetic- activated cell sorting [193, 194, 238], would be beneficial towards identifying these specific changes. However, the low yield of such techniques combined with the high protein input requirement of the Orbitrap mass spectrometer rendered such a level of resolution unfeasible in the current experiment.

Sample preparation for mass spectrometry

Preparation of the samples for mass spectrometry involved running P2+M samples on SDS gradient gels and subsequently cutting each gel into 12 pieces. This was performed in order to reduce the overall complexity of each sample and to facilitate the detection of mass spectra from as many peptides as possible. Although every effort was made to standardize the way in which the gel was cut, minute differences in the duration of the electrophoresis or imprecisions while cutting would result in a slightly different subset of proteins being present in each slice. The effects of these deviations would result in shifts of protein populations during the HPLC elution and could consequently affect the mass spectrometer's ability to detect and quantify the corresponding peptides as only the top 5 most abundant peaks per scan were selected for MS-MS (i.e., via data dependent acquisition). Another consequence of the large number of slices is that samples had to be analyzed over a period of several weeks, in which fluctuations in the mass spectrometer's performance and sensitivity might have induced measurement aberrations.

Possibilities to improve the experimental design

Alterations can be made to the currently employed experimental protocol to reduce both technical and biological variation in order to achieve the desired astrocyte-specific plastic protein profile. In order to reduce biological variation, an *ex-vivo* model can be substituted for the lactating and hyperosmotic rats. The same structural plasticity observed in the SON

during hyperosmosis and lactation can be induced in acute hypothalamic slices from pregnant rats with the joint application of oxytocin and hyperosmotic medium [236]. The ability to precisely time the application of the stimulus would allow for increased consistency in protein expression between samples. Additionally, one half of the slice could be used as a control (virgin) and the other half treated with the conditioned medium, so that each animal can act as its own control for even more accurate measurements of protein level changes.

Advances in mass spectrometry technology have also made it possible to now quantify a large number of proteins using a smaller amount of input. Using a more sensitive mass spectrometer than the one utilized in this study, it is possible to quantify more than 3000 proteins from only 5 µg of protein, compared with the 50 µg used here (Chapter 3). This very low input requirement means it will be possible to process the samples into sucrose synaptosomes, instead of a crude membrane fraction, to obtain a more precise overview of protein level changes specifically at the synapse. Furthermore, the in-gel digestion procedure requires the gel to be cut into only 2 slices thereby dramatically diminishing technical variation. The decreased number of slices also means the entire analysis time is limited so there is less opportunity for fluctuations in mass spectrometer performance to occur during the data acquisition.

Combining the reduced biological variation of precisely timed acute slices with cutting edge, high-sensitivity mass spectrometry can overcome the hurdles faced here to further our knowledge of the underlying mechanisms of astrocyte plasticity in the SON. The results of an improved mass spectrometry screen could confirm the up-regulation of Ndrg2 by SON stimulation, as well as identify additional target proteins. Interference with expression of

Ndrg2 may impair astrocyte retraction and subsequently induce deficits in synaptic transmission in the SON, thus confirming its role in SON functional plasticity.

EXPERIMENTAL PROCEDURES

Induction of hyperosmotic and lactating conditions

Virgin female random-cycling Wistar Han rats (Charles River, the Netherlands) and pregnant Wistar Han rats (+/- E15, Harlan, the Netherlands) were used. All rats were 3-4 months of age. Animals were housed on a 12 hour light/dark cycle and given access to standard lab chow and water *ad libidum*. All animals were sacrificed between 13.00h -17.00h. All experiments were conducted with approval of the Animal Users Care Committee of the VU University Amsterdam.

After 2 weeks of acclimation after arrival in the animal facility, rats in the hyperosmotic group (Charles River) had their water replaced with 2% NaCl water for 7-9 days. This protocol has previously been shown to induce hyperosmosis [217]. Pregnant rats were allowed to give birth and nurse litters for 12-15 days. Virgin rats were housed in the same room and left undisturbed.

Isolation of supraoptic nuclei from acute slices

Rats were decapitated by guillotine without anesthesia, as anesthetics have been shown to alter synapse physiology [239]. Brains were rapidly removed and chilled in an ice-slurry of artificial cerebrospinal fluid (aCSF, 125 NaCl, 3 KCl, 1.25 NaH_2PO_4, 1 $MgSO_4$, 1 $CaCl_2$, 10 glucose) for 1 min. The brain was roughly cut with a razor blade into a block containing the hypothalamus and then quickly submerged in a chilled vibrotome bath (Leica) with ice-cold carbogenated (95% O_2, 5% CO_2) aCSF. Using the optic chiasm as a guide, a 1 mm thick slice

was cut which contained the SON. The slice was placed in a Petri dish with cold aCSF on ice and a punch of tissue, 1 mm in diameter containing the SON, was removed from each hemisphere [237]. The tissue punches were immediately frozen on dry ice.

P2+microsome (P2+M) isolation

Due to the small size of the supra optic nucleus, SON from 3 animals were pooled to generate each sample. Frozen (-80°C) SON were homogenized in ice-cold 0.32M sucrose/5 mM HEPES with added protease inhibitors (Roche). The homogenate was spun down at 1000x g for 10 min. to remove nuclei and cell debris. The resulting supernatant was then pelleted by ultracentrifugation at 30,000 RPM for 2 hours. The pellet (P2+M fraction) was resuspended in 25 mM HEPES and protein concentration of each sample was determined by Bradford assay (Biorad). Samples were stored at -80°C until further use. Ten P2+M samples were generated for each experimental condition, 4 to be used for mass spectrometry and 6 for immunoblot validations.

In-gel digestion

Four virgin, lactating, and hyperosmotic samples were analyzed by mass spectrometry. The protocol was performed as previously [199], with some modifications. For each sample, 50 ug of the P2+M sample was mixed with SDS sample buffer and denatured for 5 minutes at 98° C. To block cysteine residues, 50 mM iodoacetamide was added to each sample and allowed to incubate for 30 minutes. Samples were run on 4-12% Bis-Tris NuPAGE gels (Thermo Fisher Scientific) in NuPAGE MOPS SDS buffer (Thermo Fisher Scientific). Gels were fixed overnight and stained with Coomassie blue to visualize all proteins. Each sample lane was cut into 12 equal sized pieces to reduce overall sample complexity. Each gel piece was further cut into ~1 mm^3 blocks and placed in a 96 well filter plate (Millipore). A collection plate (Eppendorf) was

placed below the filter plate so that, after spinning plates for 1 minute at 200x g, waste solutions could easily be discarded. A fresh collection plate was used for the peptide elution phase. Destaining of the gel slices was achieved by two rounds of incubation in 50% acetonitrile/ 50 mM ammonium bicarbonate, dehydration by 100% acetonitrile, and rehydration in 50 mM ammonium bicarbonate. After the second acetonitrile dehydration gel pieces were rehydrated in 50 mM ammonium bicarbonate containing 10 ug/ mL of sequence grade trypsin (Promega) and incubated at 37 °C overnight. Peptides were extracted from the gel pieces with 3, 30 minute rounds of incubation in 50% acetonitrile/ 0.1% Trifluoroacetic acid. The extracted peptide solution was dried in a SpeedVac and stored at -20°C until mass spectrometry analysis.

HPLC-Orbitrap MS/MS

Peptides were re-dissolved in 0.1% acetic acid and injected into an Eksigent HPLC system coupled to an LTQ-Orbitrap mass spectrometer (Thermo Electron, San Jose, CA, USA). Samples were initially trapped on a 5 mm Pepmax 100 C18 column (Dionex, 100 µm ID, 5 µm particle size) and then analyzed on a 200 mm Alltima C18 homemade column (100 µm ID, 3 µm particle size). Separation was achieved using a mobile phase from 5% acetonitrile, 94.9% H_2O, 0.1% acetic acid (Phase A) and 95% acetonitrile, 4.9% H20, 0.1 acetic acid (phase B), and a linear gradient from 5% to 40% buffer B for 40 min. at a flow rate of 400 nL/min. The LTQ Orbitrap mass spectrometer was operated in data dependent mode, in which one full-scan survey MS experiment (m/z range 330-2000) was followed by MS-MS experiments on the 5 most abundant ions.

Peptide matching and quantitation

MaxQuant software (version 1.3.0.2) was used for spectrum annotation and relative protein quantification [201]. Spectra were annotated against the Uniprot rat reference proteome database (version 11-2012). Enzyme specificity was set to Trypsin/ P (normal trypsin cut, disallows cutting when the site is before a proline residue), while allowing for at most two missed cleavages. Carbamidomethylcysteine was set as a fixed modification, and N-acetylation and methionine oxidation were set as variable modifications. False-discovery rate cutoffs for peptide and protein identifications were 5%. Mass deviation tolerance was set to 20 ppm for mono-isotopic precursor ions and 0.5 Da for MS-MS peaks. The minimum peptide length was seven amino acids. When a protein was identified that has the same set of peptides or a subset of peptides compared with another protein, these proteins were merged into a protein group. Only proteins or protein groups are reported when at least a single unique peptide has been observed. Peptides that are shared between different proteins or protein groups that have unique peptide evidence, are assigned to the protein/protein group that has most peptide evidence. Label-free protein quantification was performed with MaxQuant LFQ intensity values. To minimize noise, LFQ intensities were only calculated when samples had at least two identical and unmodified peptides that could be used for ratio calculation.

Mass spectrometry data analysis

Before statistical evaluation, proteins were filtered according to the times a MaxQuant LFQ intensity value was available for respective proteins; only proteins present in at least 2 samples of a single experimental group were included. To evaluate whether significant changes in protein expression occurred between experimental conditions, LFQ intensity

values were subjected to Significance Analysis of Microarrays (SAM) analysis to derive permutation-based false discovery rates (FDR) [240]. Statistical analysis was performed in both multiclass (virgin, lactating, hyperosmotic) and pair-wise (virgin *vs*. lactating and virgin *vs*. hyperosmotic) designs.

Hierarchical clustering

Hierarchical clustering was performed on a subset of proteins that adhere to 22% FDR of differential protein expression.

For clustering of samples, protein LFQ intensity values were centered, and clustering was performed using a Pearson correlation coefficient-derived distance and the average-linkage method of agglomeration.

For clustering of proteins, protein LFQ intensity values were centered/scaled, and clustering was performed using Euclidean distance and Ward's method of agglomeration. The sixteen protein plasticity clusters were arbitrarily defined by cutting the protein-relationship dendrogram at a height that resulted in appropriate aggregation of related protein expression profiles.

Gene ontology analysis

For the gene ontology analysis the Bingo plug-in (v2.44) for Cytoscape (v2.8.3) was used to perform a hypergeometric test to assess over-representation of GO terms for biological process. Statistically significant ($p \leq 0.005$ after correction with Benjamini and Hochberg False discovery Rate) over-representation of GO terms was derived from comparison with the built-in reference set of all annotated rat genes.

Immunoblotting

Mass spectrometry immunoblotting validations were performed on 5 independent replicates of P2+M from virgin, lactating, and hyperosmotic animals. Proteins were diluted in SDS sample buffer and denatured by heating to 98° C for 5 min. Five micrograms of each sample were separated on Criterion 4-15% TGX Stain-Free precast gradient polyacrylamide gels (BioRad) and transferred to PVDF membrane (BioRad). Membranes were blocked in 5% skim milk-Tris-buffered saline/ 0.05% Tween 20 (TBS-T) and incubated overnight with primary antibody at 4 °C. Primary antibodies used were against Ezrin (1:1,000, GenScript), Ndrg2 (1:200, Santa Cruz), Aldoc (1:1,000, Santa Cruz), Atp1a2 (1:5,000, Millipore), Ppap2b (1:1,000, a kind gift from Dr. Andrew Morris, University of Kentucky, USA), Aqp4 (1:200, Abcam), Intersectin1 (1:500, a kind gift from Dr. Oleg Shupaliakov, Karolinska Institute, Sweden), Slc6a11 (1:500, Abcam) Ptprf (1:200, Neuromab), PDI(1:500, Santa Cruz), NSF (1:500, Genscript), Pdia3 (1:500, Santa Cruz), and TH (1:500, Millipore).

Probed membranes were incubated with SuperSignal West Femto Chemiluminescent substrate (Thermo-Scientific) and the reaction was imaged with a Li-Cor Odyssesy 2800 scanner. Blots were quantified using ImageStudio with background correction. To visualize initial protein loading for quantification normalization, gels were activated with UV-light prior to transfer using Gel Doc EZ Imager. ImageLab was used to quantify the optical density of the total protein content of each sample on the gel which was used as a loading control for the corresponding immunoblot.

Statistical analyses were performed with SPSS 21 (IBM). Immunoblot validations were analyzed by one-way ANOVA and subsequent *post-hoc* analysis was performed with Fisher's least significant difference (LSD) test.

ACKNOWLEDGEMENTS

We would like to thank J.M. Israel and A.J. Timmerman for their assistance with the SON dissections. KEC was sponsored by the Erasmus Mundus ENC Network, the University of Bordeaux and Vrije University. PvN and ABS received support from HEALTH-2009-2.1.2-1 EU-FP7 'SynSys' (#242167). SHRO is supported by Inserm, University of Bordeaux and La Fondation pour la Recherche Médicale (Equipe FRM).